SOLUTION OF ONE-DIMENSIONAL BURGERS EQUATION USING FINITE VOLUMES AND INTEGRAL TRANSFORMS

D. J. N. M. Chalhub, dchalhub@gmail.com
L. A. Sphaier, lasphaier@id.uff.br
Laboratório de Mecânica Teórica e Aplicada, Programa de Pós-Graduação em Engenharia Mecânica, Universidade Federal Fluminense, Rua Passo da Pátria 156, bloco E, sala 216, Niterói, RJ, 24210-240, Brazil
L. S. de B. Alves, leonardo_alves@ime.eb.br
Laboratório de Motores e Propulsão, Departamento de Engenharia Mecânica e de Materiais, Instituto Militar de Engenharia, Praia Vermelha 80, Rio de Janeiro, RJ 22290-270, Brazil.

Abstract. *Both fully numerical discretization-based methods and hybrid analytical-numerical methods have been proven effective for solving advection-diffusion problems; nevertheless, each type of methodology possesses inherent characteristics that may be better suited for different type of applications. Under this scenario, this paper proposes a comparison between a traditional discretization-based mehtod – the Finite Volume Method (FVM) and the well-established hybrid-numerical approach know as the Generalized Integral Transform Technique (GITT). This paper proposes a comparison between both approaches for the solution of a one-dimensional problem in which both advection and diffusion are present: Burgers Equation. Computational implementations using different discretization approaches for the FVM and different filtering options for the GITT are developed. All time-integration is handled using the same initial value problem (IVP) integration routine, in order to provide a consistent comparison. Numerical results are calculated for different Reynolds numbers, and a comparative analysis is performed, showing which method is more suitable for each condition.*

Keywords: *Integral Transform, Convection-Diffusion, Fluid Flow*

1. NOMENCLATURE

Nomenclature

L	domain length
u	dimensional velocity
U	dimensionless velocity
Re	Reynolds number
Greek Symbols	
μ	eigenvalues
ν	momentum diffusivity
ψ	eigenfunctions
$\tilde{\psi}$	normalized eigenfunctions
τ	dimensionless time
ξ	dimensionless spatial coordinate

Subscripts	
in	inlet
k	index for different equations and unknowns
Superscripts	
$(\ )_H$	filtered quantity

2. INTRODUCTION

For a long time, analytical techniques were the only available methods for solving diffusion and convection-diffusion problems. Naturally, only a restricted and simplified class of problems could be handled, mostly involving only linear problems. Numerical methods based on domain discretization also originated years ago, but its large-scale application as well as its effective development took place in a recent past, after the availability of high-speed computing equipment. Classical examples of such techniques are the Finite Volume Method (Patankar, 1980) and the Finite Difference Method (Anderson *et al.*, 1984). Hybrid alternatives, combining analytical and numerical schemes, such as the Generalized Integral Transform Technique (Cotta, 1993), are relatively new methods, which have been successfully applied to a series of convection-diffusion problems. Both approaches, fully numerical and hybrid methods are proven to be effective for solving convection-diffusion problems. Nevertheless, each alternative possesses inherent characteristics that may be better suited for different type of applications. For instance, integral transform solutions have been shown to be extremely effective for tackling dominantly diffusive problems. On the other hand, discrete approaches have been shown to be well suited for handling advection dominant problems, particularly when advanced upwind discretization techniques are employed.

Some of the most recent applications of the Generalized Integral Transform Technique include, convective heat transfer in flows within wavy walls (Castellões *et al.*, 2010), hyperbolic heat conduction problems (Monteiro *et al.*, 2009), conjugated conduction-convection problems (Naveira *et al.*, 2009), transient diffusion in heterogeneous media (Naveira-Cotta *et al.*, 2009), heat and mass transfer in adsorption (Hirata *et al.*, 2009), atmospheric pollutant dispersion (Almeida *et al.*, 2008) and dispersion in rivers and channels (de Barros and Cotta, 2007), heat transfer in Magnetohydrodynamics (MHD) (Lima *et al.*, 2007), applications to irregular geometries (Sphaier and Cotta, 2002), solution of the Navier-Stokes equations (de Lima *et al.*, 2007) and the boundary layer equations (Paz *et al.*, 2007), stability analysis in natural convection (de B. Alves *et al.*, 2002), among others. One particularly interesting study was that proposed in (Sphaier *et al.*, 2011), in which a unified algorithm (termed the UNIT algorithm) for handling virtually any convection-diffusion problem was introduced.

Although there are a number of studies dedicated to solving convection-diffusion problems by fully-discrete or eigenfunction-based methods, there is a relative lack of comparative studies. Among these, one should mention (Chalhub *et al.*, 2008) and (Chalhub and Sphaier, 2009), which compared FVM and GITT solutions for the problem of thermally developing flow between parallel plates, for Newtonian and Non-Newtonian fluids, respectively. Furthermore (Chalhub and Sphaier, 2010, 2011) presented similar comparisons for the multidimensional thermally developing flow within a rectangular duct. The latter study presented a combined discrete-eigenfunction expansion based solution strategy by solving the flow problem by FVM and the thermal problem by GITT, and vice-versa. In spite of the relevance of the previously mentioned studies, all of them compared GITT and discrete methodologies for solving steady-state problems with diffusion effects occurring perpendicularly to the flow (advective) direction. The current study proposes a comparison between integral-transform and finite-volume solutions for a classic one-dimensional transient problem that involves both advection and diffusion in the same direction: Burgers Equation for one-dimensional fluid flow. The presented results are aimed at evaluating how each methodology performs for problems that are more diffusive (lower Reynolds values) and more advective (higher Reynolds values).

3. PROBLEM FORMULATION

The considered problem is described by Burgers equation in a one-dimensional form with Dirichlet boundary conditions, as given below:

$$\frac{\partial U}{\partial \tau} + U\,\frac{\partial U}{\partial \xi} = \frac{1}{\mathrm{Re}}\,\frac{\partial^2 U}{\partial \xi^2}, \qquad \text{in} \quad 0 \le \xi \le 1, \quad \text{for} \quad \tau \ge 0, \tag{1a}$$

$$U(0,\tau) = 1, \quad \text{for} \quad \tau > 0, \tag{1b}$$

$$U(1,\tau) = 0, \quad \text{for} \quad \tau > 0, \tag{1c}$$

$$U(\xi,0) = 0, \qquad \text{in} \quad 0 \le \xi \le 1, \tag{1d}$$

where the dimensionless variables and parameters are given by:

$$\mathrm{Re} = \frac{u_{in}\,L}{\nu}, \qquad U = \frac{u}{u_{in}}, \qquad \xi = \frac{x}{L}, \qquad \tau = \frac{t\,u_{in}}{L} \tag{2a}$$

4. GITT SOLUTION

In order to solve the proposed problem using the GITT, a filter is used due to the non-homogeneous boundary terms:

$$U(\xi,\tau) = U_F(\xi) + U_H(\xi,\tau), \qquad \text{with} \qquad U_F(0) = 1, \qquad U_F(1) = 0. \tag{3}$$

The resulting filtered problem is then given by:

$$\frac{\partial U_H}{\partial \tau} + (U_H + U_F)\,\frac{\partial U_H}{\partial \xi} + U_H\,\frac{\mathrm{d} U_F}{\mathrm{d}\xi} = \frac{1}{\mathrm{Re}}\,\frac{\partial^2 U_H}{\partial \xi^2} + P(\xi), \tag{4a}$$

$$U_H(0,\tau) = 0, \tag{4b}$$

$$U_H(1,\tau) = 0, \tag{4c}$$

$$U_H(\xi,0) = -U_F(\xi), \tag{4d}$$

where the non-homogeneous term that is introduced in the differential equation due to filtering is given by:

$$P(\xi) = \left(\frac{1}{\mathrm{Re}}\,\frac{\mathrm{d}^2 U_F}{\mathrm{d}\xi^2} - U_F\,\frac{\mathrm{d} U_F}{\mathrm{d}\xi}\right) \tag{5}$$

The general form given by eq. (3) allows a variety of filters. In this study four different possibilities were tested, as described below:

- Linear Filter (LF):

$$0 = \frac{1}{\mathrm{Re}}\,\frac{\mathrm{d}^2U_F}{\mathrm{d}\xi^2} \quad \rightarrow \quad U_F(\xi) = 1-\xi \tag{6}$$

- Linearized Steady Filter (LSF):

$$\frac{\mathrm{d}U_F}{\mathrm{d}\xi} = \frac{1}{\mathrm{Re}}\,\frac{\mathrm{d}^2U_F}{\mathrm{d}\xi^2} \quad \rightarrow \quad U_f = \frac{\exp(\mathrm{Re})-\exp(\mathrm{Re}\,\xi)}{\exp(\mathrm{Re})-1} \tag{7}$$

- Linear Velocity Steady Filter (LVSF):

$$(1-\xi)\,\frac{\mathrm{d}U_F}{\mathrm{d}\xi} = \frac{1}{\mathrm{Re}}\,\frac{\mathrm{d}^2U_F}{\mathrm{d}\xi^2} \quad \rightarrow \quad U_f = \frac{\mathrm{erf}(\sqrt{\mathrm{Re}/2}\,(\xi-1))}{\mathrm{erf}(\sqrt{\mathrm{Re}/2})} \tag{8}$$

- Real Steady Filter (RSF):

$$\frac{1}{2}\,\frac{\mathrm{d}U_F^2}{\mathrm{d}\xi} = \frac{1}{\mathrm{Re}}\,\frac{\mathrm{d}^2U_F}{\mathrm{d}\xi^2} \quad \rightarrow \quad U_f = -\frac{2\,a}{\mathrm{Re}}\,\tanh\big(a\,(b+\xi)\big), \tag{9a}$$

  in which the coefficients a and b depend on the Reynolds number via the relations below:

$$\tanh(a) = \frac{\mathrm{Re}}{2\,a}, \qquad \tanh(a\,b) = -\frac{\mathrm{Re}}{2\,a}. \tag{9b}$$

After filtering the following eigenvalue problem is selected for the GITT solution:

$$\psi'' + \mu^2\,\psi = 0, \qquad \psi(0) = 0, \qquad \psi(1) = 0, \tag{10}$$

in which the eigenfunctions ψ possesses the following ortho-normality property:

$$\int_0^1 \tilde{\psi}_n(\xi)\,\tilde{\psi}_m(\xi)\,\mathrm{d}\xi = \delta_{n,m}, \tag{11}$$

where $\delta_{n,m}$ is the Kronencker delta function. Based on this relation, the following integral transform pair is obtained:

$$U_H = \sum_{n=1}^{\infty} \bar{U}_n(\tau)\,\tilde{\psi}_n(\xi), \qquad \bar{U}_n(\xi) = \int_0^1 U_H(\xi,\tau)\,\tilde{\psi}_n(x)\,\mathrm{d}\xi. \tag{12a}$$

4.1 Problem transformation

The problem transformation begins by multiplying equation (4a) by the eigenfunction and integrating within the problem domain:

$$\int_0^1 \frac{\partial U_H}{\partial \tau}\,\tilde{\psi}\,\mathrm{d}\xi + \int_0^1 \left((U_H+U_F)\,\frac{\partial U_H}{\partial \xi} + U_H\,\frac{\mathrm{d}U_F}{\mathrm{d}\xi}\right)\tilde{\psi}\,\mathrm{d}\xi = \frac{1}{\mathrm{Re}}\int_0^1 \frac{\partial^2 U_H}{\partial \xi^2}\,\tilde{\psi}_n\,\mathrm{d}\xi + \int_0^1 P(\xi)\,\tilde{\psi}\,\mathrm{d}\xi, \tag{13}$$

leading to the following form after the substitution of the integral transformation:

$$\frac{\mathrm{d}\bar{U}_n}{\mathrm{d}\tau} + \int_0^1 \left((U_H+U_F)\,\frac{\partial U_H}{\partial \xi} + U_H\,\frac{\mathrm{d}U_F}{\mathrm{d}\xi}\right)\tilde{\psi}_n\,\mathrm{d}\xi = -\frac{1}{\mathrm{Re}}\,\mu_n^2\,\bar{U}_n + \bar{P}_n. \tag{14}$$

Then, substituting the inversion formula into the non-transformable terms leads to:

$$\frac{\mathrm{d}\bar{U}_n}{\mathrm{d}\tau} + \sum_{m=1}^{\infty}\sum_{l=1}^{\infty} A_{n,m,l}\,\bar{U}_m\,\bar{U}_l + \sum_{m=1}^{\infty} B_{n,m}\,\bar{U}_m = -\frac{1}{\mathrm{Re}}\,\mu_n^2\,\bar{U}_n + \bar{P}_n, \tag{15}$$

in which the integral coefficients are given by:

$$A_{n,m,l} = \int_0^1 \tilde{\psi}_n\,\tilde{\psi}_m\,\tilde{\psi}_l'\,\mathrm{d}\xi, \qquad B_{n,m} = \int_0^1 \tilde{\psi}_n\,(U_F\,\tilde{\psi}_m' + U_F'\,\psi_m)\,\mathrm{d}\xi, \qquad \bar{P}_n = \int_0^1 \tilde{\psi}_n\,P\,\mathrm{d}\xi. \tag{16a}$$

Finally, the transformation of the initial condition leads to:

$$\bar{U}_n(0) = \bar{f}_n = -\int_0^1 U_F\,\tilde{\psi}_n\,\mathrm{d}\xi. \tag{17}$$

System (15)-(17) is then solved using the numeric ODE solver **NDSolve** available in the *Mathematica* system. After this numerical solution, the original velocity is obtained using the inversion formula together with the filter function:

$$U(\xi,\tau) = U_F(\xi) + \sum_{n=1}^{\infty} \bar{U}_n(\tau)\,\tilde{\psi}_n(\xi). \tag{18}$$

5. FINITE VOLUME METHOD

The solution of the studied problem via finite volumes begins by integrating eq. (1a) in conservative form within a finite volume of size $\Delta\xi = 1/I$, leading to:

$$\frac{\partial}{\partial \tau}\int_{\xi_w}^{\xi_e} U\,\mathrm{d}\xi + \frac{1}{2}(U^2|_{\xi_e} - U^2|_{\xi_w}) = \frac{1}{\mathrm{Re}}\left(\left.\frac{\partial U}{\partial \xi}\right|_{\xi_e} - \left.\frac{\partial U}{\partial \xi}\right|_{\xi_w}\right), \tag{19}$$

which can be rearranged in the form:

$$\frac{\mathrm{d}}{\mathrm{d}\tau}\int_{\xi_w}^{\xi_e} U\,\mathrm{d}\xi + \frac{1}{2}(U|_{\xi_e} + U|_{\xi_w})(U|_{\xi_e} - U|_{\xi_w}) = \frac{1}{\mathrm{Re}}\left(\left.\frac{\partial U}{\partial \xi}\right|_{\xi_e} - \left.\frac{\partial U}{\partial \xi}\right|_{\xi_w}\right). \tag{20}$$

where traditional finite-volume coordinates (P, E, W, e and w) are employed.

Then, a second-order approximations are employed for integration and for interpolating the velocity (but not the difference term) in the advective term:

$$\int_{\xi_w}^{\xi_e} U\,\mathrm{d}\xi \approx \Delta\xi\, U_P, \qquad \frac{1}{2}(U|_{\xi_e} + U|_{\xi_w}) \approx U_P \tag{21}$$

leading to the following form:

$$\frac{\mathrm{d}U_P}{\mathrm{d}\tau} + U_P\,\frac{U|_{\xi_e} - U|_{\xi_w}}{\Delta\xi} = \frac{1}{\mathrm{Re}\,\Delta\xi}\left(\left.\frac{\partial U}{\partial \xi}\right|_{\xi_e} - \left.\frac{\partial U}{\partial \xi}\right|_{\xi_w}\right). \tag{22}$$

Then, second-order central-differencing (CDS) approximations can be employed for the remaining interpolation:

$$U|_{\xi_e} \approx \frac{U_E + U_P}{2}, \qquad U|_{\xi_w} \approx \frac{U_P + U_W}{2}, \qquad \left.\frac{\partial U}{\partial \xi}\right|_{\xi_e} \approx \frac{U_E - U_P}{\Delta\xi}, \qquad \left.\frac{\partial U}{\partial \xi}\right|_{\xi_w} \approx \frac{U_P - U_W}{\Delta\xi}, \tag{23a}$$

Alternatively, a simple first-order upwind differencing scheme (UDS) can be used for the advective derivative:

$$\frac{U|_{\xi_e} - U|_{\xi_w}}{\Delta\xi} \approx \frac{U_P - U_W}{\Delta\xi}. \tag{23b}$$

The boundary conditions are employed in the inlet and outlet, such that the following approximations are obtained for the advective and diffusive derivatives in cells adjacent to those positions:

$$\text{inlet, CDS} \implies \frac{U|_{\xi_e} - U|_{\xi_w}}{\Delta\xi} \approx \frac{(U_P + U_E)/2 - 1}{\Delta\xi}, \qquad \left.\frac{\partial U}{\partial \xi}\right|_{\xi_w} \approx \frac{U_P - 1}{\Delta\xi/2}, \tag{24a}$$

$$\text{outlet, CDS} \implies \frac{U|_{\xi_e} - U|_{\xi_w}}{\Delta\xi} \approx \frac{0 - (U_W + U_P)/2}{\Delta\xi}, \qquad \left.\frac{\partial U}{\partial \xi}\right|_{\xi_e} \approx \frac{0 - U_P}{\Delta\xi/2}, \tag{24b}$$

$$\text{inlet, UDS} \implies \frac{U|_{\xi_e} - U|_{\xi_w}}{\Delta\xi} \approx \frac{U_P - 1}{\Delta\xi/2}, \qquad \left.\frac{\partial U}{\partial \xi}\right|_{\xi_w} \approx \frac{U_P - 1}{\Delta\xi/2}, \tag{24c}$$

$$\text{outlet, UDS} \implies \frac{U|_{\xi_e} - U|_{\xi_w}}{\Delta\xi} \approx \frac{U_P - U_W}{\Delta\xi}, \qquad \left.\frac{\partial U}{\partial \xi}\right|_{\xi_e} \approx \frac{0 - U_P}{\Delta\xi/2}. \tag{24d}$$

Then, the following mapping is employed to translate the FVM coordinates into a computational index:

$$P = i, \qquad W = i - 1, \qquad E = i + 1, \tag{25}$$

which allows the discretized system to be written in the following general form:

$$\frac{\mathrm{d}U_i}{\mathrm{d}\tau} = F_i(U_1, U_2, \ldots, U_I, \tau), \qquad U_i(0) = 0, \tag{26}$$

for $i = 1, 2, \ldots, I$. The F-functions, which carry all the discretization information, are given by, for CDS:

$$F_i = -U_i\,\frac{U_{i+1} - U_{i-1}}{2\,\Delta\xi} + \frac{(U_{i+1} - 2\,U_i + U_{i-1})}{\mathrm{Re}\,\Delta\xi^2}, \qquad \text{for} \quad 2 \le i \le I - 1 \tag{27a}$$

$$F_1 = -U_1\,\frac{U_1 + U_2 - 2}{2\,\Delta\xi} + \frac{2 - 3\,U_1 + U_2}{\mathrm{Re}\,\Delta\xi^2} \tag{27b}$$

$$F_I = -U_I\,\frac{0 - (U_{I-1} + U_I)}{2\,\Delta\xi} + \frac{U_{I-1} - 3\,U_I}{\mathrm{Re}\,\Delta\xi^2} \tag{27c}$$

and for UDS:

$$F_i = -U_i \frac{U_i - U_{i-1}}{\Delta\xi} + \frac{(U_{i+1} - 2U_i + U_{i-1})}{\mathrm{Re}\,\Delta\xi^2}, \qquad \text{for} \quad 2 \le i \le I-1 \tag{28a}$$

$$F_1 = -U_1 \frac{U_1 - 1}{\Delta\xi/2} + \frac{2 - 3U_1 + U_2}{\mathrm{Re}\,\Delta\xi^2} \tag{28b}$$

$$F_I = -U_I \frac{U_I - U_{I-1}}{\Delta\xi} + \frac{U_{I-1} - 3U_I}{\mathrm{Re}\,\Delta\xi^2} \tag{28c}$$

Similarly to what was done for the GITT solution, the system of ODEs arising from discretization is then solved using the *Mathematica* **NDSolve** function.

6. RESULTS AND DISCUSSION

After describing the adopted solution schemes, numerical results from the computational implementations are presented. Tables 1 and 2 present the FVM convergence for with the number of grid divisions, I for CDS and UDS solutions, respectively, for $\mathrm{Re} = 1$ and $\tau = 1$. As can be seen, the UDS convergence is clearly (as expected) worse than the CDS, with the former presenting six converged figures for 100 grid-divisions and the latter not fully converged (with six figures) with 12800 divisions. The main reason for this difference is the lower order of the employed UDS when compared to the CDS.

Table 1. FVM-CDS Results for $\mathrm{Re} = 1$ and $\tau = 1$: velocity at different positions.

	position, ξ					
I	0.1	0.3	0.5	0.7	0.9	CPU(s)
6	0.928948	0.761388	0.567462	0.351067	0.119049	0.00
12	0.927488	0.761426	0.567546	0.351205	0.118871	0.02
25	0.927534	0.761193	0.567684	0.351090	0.118876	0.05
50	0.927394	0.761059	0.567571	0.351015	0.118849	0.13
100	0.927394	0.761060	0.567573	0.351016	0.118850	0.20
200	0.927394	0.761060	0.567573	0.351016	0.118850	0.42
400	0.927394	0.761060	0.567573	0.351016	0.118850	0.90
800	0.927394	0.761060	0.567573	0.351016	0.118850	1.86
1600	0.927394	0.761060	0.567573	0.351016	0.118850	4.35
3200	0.927394	0.761060	0.567573	0.351016	0.118850	11.30
6400	0.927394	0.761060	0.567573	0.351016	0.118850	27.19
12800	0.927394	0.761060	0.567573	0.351016	0.118850	57.66

Table 2. FVM-UDS Results for $\mathrm{Re} = 1$ and $\tau = 1$: velocity at different positions.

	position, ξ					
I	0.1	0.3	0.5	0.7	0.9	CPU(s)
6	0.927350	0.758060	0.563929	0.348513	0.118138	0.02
12	0.926709	0.759714	0.565730	0.349892	0.118406	0.03
25	0.927154	0.760363	0.566797	0.350452	0.118649	0.05
50	0.927204	0.760642	0.567125	0.350694	0.118735	0.11
100	0.927299	0.760851	0.567349	0.350855	0.118793	0.20
200	0.927347	0.760955	0.567461	0.350935	0.118821	0.45
400	0.927371	0.761008	0.567517	0.350976	0.118836	1.48
800	0.927382	0.761034	0.567545	0.350996	0.118843	2.09
1600	0.927388	0.761047	0.567559	0.351006	0.118846	5.98
3200	0.927391	0.761054	0.567566	0.351011	0.118848	13.25
6400	0.927393	0.761057	0.567569	0.351014	0.118849	30.05
12800	0.927394	0.761059	0.567571	0.351015	0.118849	62.01

Next, table 3 presents the convergence of the GITT solutions, for all of the considered filters, with the truncation order $n_{\max}$. As one can clearly observe, for the GITT solutions, convergence behavior strongly depends on the adopted filter. The RSF is clearly superior than the other filters providing a fully six-digit converged solution with about five terms. This superiority can be explained by the fact that this filter comprises the actual non-linear steady-state solution, and that the considered dimensionless time is not far from the steady-state regime. The second-to-best filter is the LVSF, yielding six-digit convergence with 50 terms near the inlet ($\xi = 0.1$ and $\xi = 0.3$) and improving the convergence rate further upstream, where less than 20 terms are enough for providing a fully converged solution at $\xi = 0.9$. Among the two other filters, both present an oscillatory convergence behavior, especially downstream; however the LSF is worse than the LF, requiring more terms for convergence and presenting oscillatory convergence upstream as well.

Comparing the GITT solutions with the FVM ones, in general, the GITT requires a smaller number of equations in the transformed ODE system (given by the truncation order $n_{\max}$) than the number of equations in the FVM-discretized ODE system (given by the number of grid divisions, I). This difference is even more pronounced when the FVM-UDS is considered or when the better converging GITT solutions are used. However, the FVM-CDS solution becomes competitive with the GITT solutions (in terms of the number of equations) if a unsuitable filter is selected.

Table 3. GITT Results for $\mathrm{Re} = 1$ and $\tau = 1$: velocity at different positions for different filters.

		position, ξ					
	$n_{\max}$	0.1	0.3	0.5	0.7	0.9	CPU(s)
LF	0	0.900000	0.700000	0.500000	0.300000	0.100000	0.00
	5	0.927069	0.761031	0.567640	0.350892	0.118969	0.09
	10	0.927470	0.761095	0.567591	0.351025	0.118853	0.27
	20	0.927380	0.761055	0.567570	0.351014	0.118849	13.99
	30	0.927399	0.761062	0.567574	0.351016	0.118850	21.95
	40	0.927392	0.761060	0.567573	0.351016	0.118850	31.12
	50	0.927396	0.761061	0.567573	0.351016	0.118850	41.81
	60	0.927394	0.761060	0.567573	0.351016	0.118850	56.13
	70	0.927395	0.761061	0.567573	0.351016	0.118850	74.38
	80	0.927394	0.761060	0.567573	0.351016	0.118850	101.78
	90	0.927395	0.761061	0.567573	0.351016	0.118850	137.92
	100	0.927394	0.761060	0.567573	0.351016	0.118850	185.14
LSF	0	0.938793	0.796390	0.622459	0.410020	0.150545	0.00
	5	0.927026	0.761317	0.567361	0.351023	0.119525	0.34
	10	0.927401	0.761042	0.567529	0.350930	0.118666	0.80
	20	0.927393	0.761063	0.567579	0.351028	0.118882	16.66
	30	0.927395	0.761060	0.567571	0.351013	0.118839	26.44
	40	0.927394	0.761061	0.567574	0.351018	0.118855	40.22
	50	0.927395	0.761060	0.567573	0.351015	0.118847	54.07
	60	0.927394	0.761061	0.567573	0.351017	0.118851	69.30
	70	0.927395	0.761060	0.567573	0.351016	0.118849	85.79
	80	0.927394	0.761061	0.567573	0.351016	0.118850	106.27
	90	0.927394	0.761060	0.567573	0.351016	0.118849	130.39
	100	0.927394	0.761060	0.567573	0.351016	0.118850	152.55
LVSF	0	0.925574	0.755941	0.560906	0.345432	0.116679	0.00
	5	0.927403	0.761061	0.567571	0.351019	0.118847	1.00
	10	0.927393	0.761060	0.567572	0.351016	0.118850	2.23
	20	0.927395	0.761061	0.567573	0.351016	0.118850	23.09
	30	0.927394	0.761060	0.567573	0.351016	0.118850	36.47
	40	0.927395	0.761061	0.567573	0.351016	0.118850	51.43
	50	0.927394	0.761060	0.567573	0.351016	0.118850	67.78
	60	0.927394	0.761060	0.567573	0.351016	0.118850	87.17
	70	0.927394	0.761060	0.567573	0.351016	0.118850	107.89
	80	0.927394	0.761060	0.567573	0.351016	0.118850	133.51
	90	0.927394	0.761060	0.567573	0.351016	0.118850	158.34
	100	0.927394	0.761060	0.567573	0.351016	0.118850	188.45
RSF	0	0.927410	0.761104	0.567630	0.351065	0.118869	0.00
	5	0.927394	0.761060	0.567573	0.351016	0.118850	0.14
	10	0.927394	0.761060	0.567573	0.351016	0.118850	0.55
	20	0.927394	0.761060	0.567573	0.351016	0.118850	19.44
	30	0.927394	0.761060	0.567573	0.351016	0.118850	30.67
	40	0.927394	0.761060	0.567573	0.351016	0.118850	43.14
	50	0.927394	0.761060	0.567573	0.351016	0.118850	57.35
	60	0.927394	0.761060	0.567573	0.351016	0.118850	73.49
	70	0.927394	0.761060	0.567573	0.351016	0.118850	92.82
	80	0.927394	0.761060	0.567573	0.351016	0.118850	113.43
	90	0.927394	0.761060	0.567573	0.351016	0.118850	137.16
	100	0.927394	0.761060	0.567573	0.351016	0.118850	162.65

The following tables present comparison results for a higher Reynolds number ($\mathrm{Re} = 10$). Tables 4 and 5 present the FVM results for $\tau = 1$ for UDS and CDS solution schemes, respectively. Again, as expected, the CDS solution performs significantly better than the UDS solution due to the higher order of the employed approximation for the advective derivative. However, when comparing with the smaller Reynolds solution, 800 divisions are required for six-digits convergence near the channel entrance ($\xi = 0.1$ and $\xi = 0.3$), and this number is gradually increased for positions upstream (up to 6400 equations for $\xi = 0.9$).

Table 4. FVM-CDS Results for $\mathrm{Re} = 10$ and $\tau = 1$: velocity at different positions.

I	position, ξ					CPU(s)
	0.1	0.3	0.5	0.7	0.9	
6	0.992561	0.905878	0.662089	0.337621	0.090384	0.02
12	0.988553	0.911974	0.692239	0.364978	0.100120	0.03
25	0.988264	0.911705	0.699858	0.373707	0.102434	0.05
50	0.987921	0.911216	0.700693	0.375883	0.103388	0.13
100	0.987906	0.911271	0.701071	0.376336	0.103529	0.25
200	0.987902	0.911285	0.701165	0.376449	0.103565	0.47
400	0.987902	0.911288	0.701188	0.376478	0.103574	1.39
800	0.987901	0.911289	0.701194	0.376485	0.103576	2.18
1600	0.987901	0.911289	0.701196	0.376487	0.103576	5.88
3200	0.987901	0.911289	0.701196	0.376487	0.103576	13.96
6400	0.987901	0.911289	0.701196	0.376487	0.103577	30.69
12800	0.987901	0.911289	0.701196	0.376487	0.103577	74.63

Table 5. FVM-UDS Results for $\mathrm{Re} = 10$ and $\tau = 1$: velocity at different positions.

I	position, ξ					CPU(s)
	0.1	0.3	0.5	0.7	0.9	
6	0.973449	0.849544	0.625818	0.343967	0.098752	0.02
12	0.978638	0.878126	0.659697	0.360474	0.102900	0.03
25	0.983506	0.894063	0.680500	0.369240	0.103351	0.06
50	0.985516	0.902019	0.690173	0.373115	0.103731	0.17
100	0.986701	0.906561	0.695573	0.374828	0.103676	0.23
200	0.987299	0.908900	0.698355	0.375664	0.103632	0.50
400	0.987600	0.910088	0.699768	0.376078	0.103606	1.50
800	0.987750	0.910687	0.700480	0.376283	0.103591	2.42
1600	0.987826	0.910988	0.700838	0.376385	0.103584	6.41
3200	0.987864	0.911138	0.701017	0.376436	0.103580	14.18
6400	0.987882	0.911214	0.701107	0.376462	0.103578	38.03
12800	0.987892	0.911251	0.701151	0.376474	0.103577	71.67

Table 6 illustrates the convergence behavior of the GITT solutions, using all proposed filters, for $\mathrm{Re} = 10$ and $\tau = 1$. As can be seen, the convergence behavior is worse than the one seen for the smaller Reynolds number. This can be justified by the increased advection/diffusion ratio; however, when looking into the steady-sate solution (given by the GITT-RSF solution with zero terms) it is also seen the dimensionless time value $\tau = 1$, in this case corresponds to a time farther from the steady-state solution, which is also responsible for giving poorer convergence rates. As a result, even for the RSF case (which yielded good convergence rates for $\mathrm{Re} = 1$), a worse performance is seen. In a general way, for $\mathrm{Re} = 10$, the LSF gives the worst convergence rates, whereas for the other filter options a similar convergence behavior is seen.

Table 6. GITT Results for $\mathrm{Re} = 10$ and $\tau = 1$: velocity at different positions for different filters.

	$n_{\max}$	position, ξ					
		0.1	0.3	0.5	0.7	0.9	CPU(s)
LF	0	0.900000	0.700000	0.500000	0.300000	0.100000	0.00
	5	0.987122	0.909687	0.698381	0.373805	0.102701	0.09
	10	0.987887	0.911069	0.700726	0.376029	0.103416	0.27
	20	0.987876	0.911248	0.701123	0.376418	0.103552	14.79
	30	0.987902	0.911280	0.701175	0.376466	0.103569	23.12
	40	0.987898	0.911284	0.701187	0.376478	0.103573	32.71
	50	0.987902	0.911287	0.701192	0.376483	0.103575	44.38
	60	0.987900	0.911288	0.701193	0.376484	0.103576	58.66
	70	0.987901	0.911288	0.701195	0.376485	0.103576	78.56
	80	0.987901	0.911289	0.701195	0.376486	0.103576	105.64
	90	0.987901	0.911289	0.701195	0.376486	0.103576	141.10
	100	0.987901	0.911289	0.701196	0.376487	0.103576	189.20
LSF	0	0.999922	0.999133	0.993307	0.950256	0.632149	0.00
	5	0.959907	0.915763	0.675385	0.370847	0.130992	0.31
	10	0.988812	0.910924	0.699196	0.371672	0.092603	0.75
	20	0.987978	0.911506	0.701579	0.377210	0.105574	18.99
	30	0.987903	0.911239	0.701078	0.376252	0.102905	30.48
	40	0.987908	0.911313	0.701241	0.376578	0.103870	43.48
	50	0.987900	0.911277	0.701169	0.376434	0.103420	58.31
	60	0.987903	0.911296	0.701209	0.376514	0.103667	73.21
	70	0.987900	0.911284	0.701186	0.376468	0.103518	91.26
	80	0.987902	0.911292	0.701202	0.376499	0.103615	114.05
	90	0.987901	0.911287	0.701191	0.376478	0.103549	136.55
	100	0.987902	0.911291	0.701199	0.376493	0.103596	157.94
LVSF	0	0.997134	0.974669	0.887543	0.658249	0.248559	0.00
	5	0.987247	0.909747	0.698439	0.373867	0.102697	0.64
	10	0.987881	0.911073	0.700734	0.376036	0.103418	1.48
	20	0.987880	0.911251	0.701126	0.376419	0.103552	21.78
	30	0.987902	0.911280	0.701176	0.376467	0.103569	34.38
	40	0.987898	0.911284	0.701187	0.376478	0.103573	48.72
	50	0.987901	0.911287	0.701192	0.376483	0.103575	64.58
	60	0.987900	0.911288	0.701193	0.376484	0.103576	83.15
	70	0.987901	0.911288	0.701195	0.376486	0.103576	103.71
	80	0.987901	0.911289	0.701195	0.376486	0.103576	128.41
	90	0.987901	0.911289	0.701196	0.376486	0.103576	152.49
	100	0.987901	0.911289	0.701196	0.376487	0.103576	182.13
RSF	0	0.999844	0.998270	0.986710	0.905255	0.462195	0.00
	5	0.982516	0.910537	0.695217	0.371974	0.106639	0.14
	10	0.987892	0.911065	0.700714	0.376008	0.103400	0.48
	20	0.987876	0.911248	0.701124	0.376418	0.103552	19.62
	30	0.987902	0.911280	0.701175	0.376466	0.103569	30.91
	40	0.987898	0.911284	0.701187	0.376478	0.103573	43.26
	60	0.987900	0.911288	0.701193	0.376484	0.103576	56.99
	50	0.987902	0.911287	0.701192	0.376483	0.103575	72.70
	70	0.987901	0.911288	0.701195	0.376485	0.103576	91.22
	80	0.987901	0.911289	0.701195	0.376486	0.103576	111.64
	90	0.987901	0.911289	0.701195	0.376486	0.103576	132.38
	100	0.987901	0.911289	0.701196	0.376487	0.103576	155.46

In order to give a better insight on the computational performance of the different types of solution schemes considered, graphics of the relative solution error against the required CPU time are plotted. Figure 1 displays the obtained results for different positions and $\mathrm{Re} = 1$. As can be seen, the FVM solutions performance have no dependence on spatial position, while the GITT solutions significantly depend on the considered location. The FVM-CDS and the GITT-RSF solutions notably have the best performance, with the FVM-CDS solution being better than the GITT-RSF solution only at $\xi = 0.3$. The FVM-UDS and the GITT-LSF have the worst performance, with the GITT solutions being better than the FVM-UDS solution for $\xi = 0.3$ and $\xi = 0.5$. The only exception is at $\xi = 0.1$, when the LF solution also performs equivalent to the FVM-UDS and the GITT-LSF solutions. The GITT-LVSF solution presents itself as a reasonable alternative, generally performing better than its LSF and LF counterparts, and approaching to the GITT-RSF and the FVM-CDS performance for some cases.

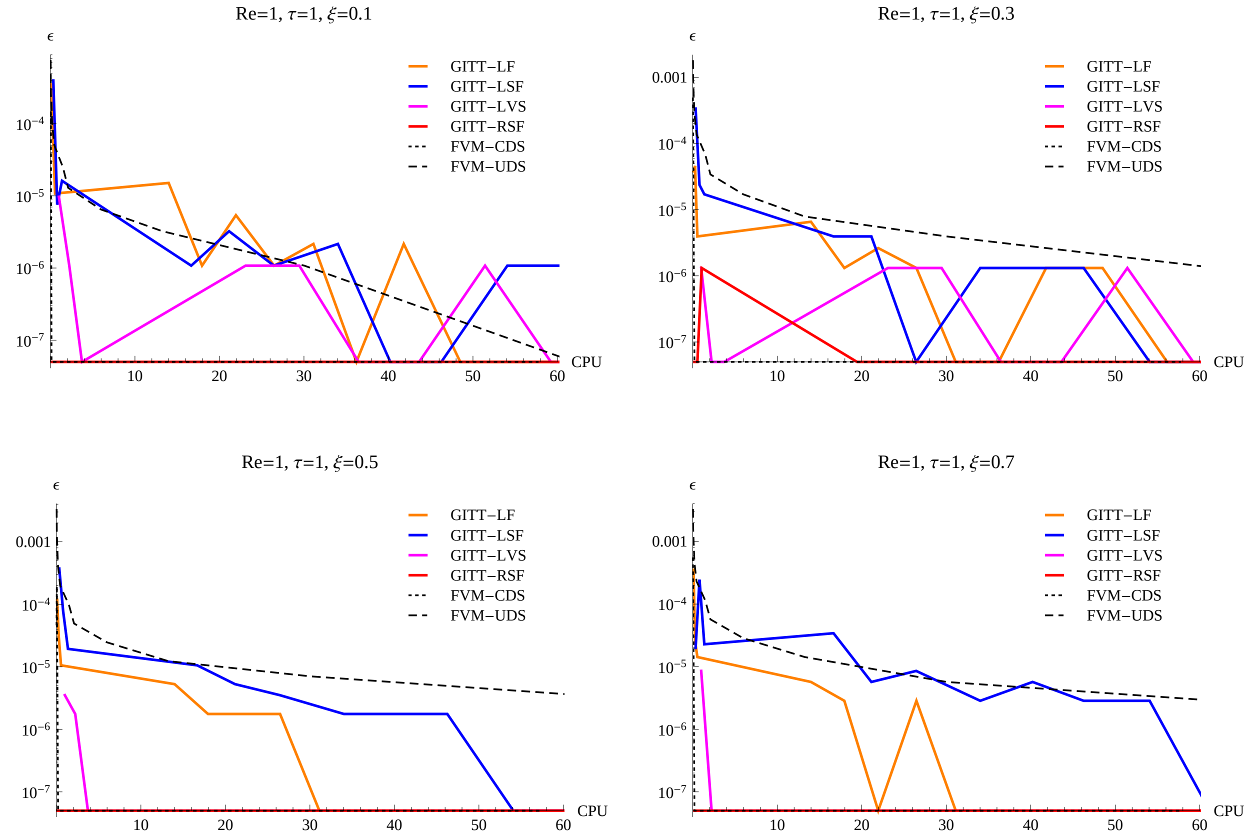

Figure 1. Solution error vs. CPU time for different GITT and FVM schemes with $\mathrm{Re} = 1$.

7. CONCLUSIONS

This paper provided an initial comparison between different solution strategies for solving the one-dimensional Burgers equation in using both the Generalized Integral Transform Technique and the Finite Volumes Method. Different solution algorithms were implemented for both methods in order to provide a reasonable amount of comparative results, and the same solution method was used for solving the resulting ODE system. For the GITT solutions four different filtering strategies were employed, whereas for the FVM two different discretization formulas for the advective term were employed. The convergence analysis results show that the GITT solutions generally require a smaller number of equations in the transformed ODE system than the number of equations in the ODE system produced by the FVM discretization. This implies that the GITT can consume less memory than the FMV one, since smaller unknown vectors are required. On the other hand, a greater CPU time *per number of equations* is seen for the GITT solutions due to the much larger number of couplings between the transformed equations. However, since the solution error with the truncation order decreases more rapidly than the FVM solution error with the grid divisions, a thorough comparison between methods must be carried-out, taking into account the solution error and the CPU time. This paper provided an initial comparing showing that the better filtered GITT solutions and CDS-FVM discretization apparently lead to a better error/CPU time ratio. However, these results are preliminary and further studies must be carried out.

8. ACKNOWLEDGEMENTS

The authors would like to acknowledge the financial support provided by, CAPES, CNPq, FAPERJ, Instituto Militar de Engenharia, and Universidade Federal Fluminense.

REFERENCES

Almeida, G.L., Pimentel, L.C.G. and Cotta, R.M., 2008. "Integral transform solutions for atmospheric pollutant dispersion". *Environmental Modeling and Assessment*, Vol. 13, No. 1, pp. 53–65.

Anderson, D.A., Tannehill, J.C. and Pletcher, R.H., 1984. *Computational Fluid Mechanics and Heat Transfer*. Taylor & Francis, 2nd edition.

Castellões, F.V., Quaresma, J.N.N. and Cotta, R.M., 2010. "Convective heat transfer enhancement in low Reynolds number flows with wavy walls". *International Journal of Heat and Mass Transfer*, Vol. 53, No. 9-10, pp. 2022–2034.

Chalhub, D.J.N.M., Dias, R.A.C., Machado, F.J.F. and Sphaier, L.A., 2008. "Comparisons between GITT and FVM solutions for thermally developing flow in parallel-plates channels". In *Proceedings of the 12th Brazilian Congress of Thermal Sciences and Engineering (ENCIT)*. Belo Horizonte, MG.

Chalhub, D.J.N.M. and Sphaier, L.A., 2009. "Analysis of finite volumes and integral transform solutions for thermally developing non-newtonian fluid flow". In *Proc. of the 3rd Southern Conference on Computational Modeling (3MCSUL)*. Rio Grande, RS, Brazil.

Chalhub, D.J.N.M. and Sphaier, L.A., 2010. "Comparisons between GITT and FVM solutions for thermally developing flow in a rectangular duct". In *Proceedings of the 13th Brazilian Congress of Thermal Sciences and Engineering (ENCIT)*.

Chalhub, D.J.N.M. and Sphaier, L.A., 2011. "Comparisons between integral transform, finite volumes and combined solution strategies for convective heat transfer problems". In *8th Thermal Engineering Joint Conference*. Honolulu, Hawaii, USA.

Cotta, R.M., 1993. *Integral Transforms in Computational Heat and Fluid Flow*. CRC Press, Boca Raton, FL.

de B. Alves, L.S., Cotta, R.M. and Pontes, J., 2002. "Stability analysis of natural convection in porous cavities through integral transforms". *International Journal of Heat and Mass Transfer*, Vol. 45, No. 6, pp. 1185–1195.

de Barros, F.P.J. and Cotta, R.M., 2007. "Integral transforms for three-dimensional steady turbulent dispersion in rivers and channels". *Applied Mathematical Modelling*, Vol. 31, pp. 2719–2732.

de Lima, G.G.C., Santos, C.A.C., Haag, A. and Cotta, R.M., 2007. "Integral transform solution of internal flow problems based on navier-stokes equations and primitive variables formulation". *International Journal for Numerical Methods in Engineering*, Vol. 69, No. 3, pp. 544–561.

Hirata, S.C., Couto, P., Lara, L.G. and Cotta, R.M., 2009. "Modeling and hybrid simulation of slow discharge process of adsorbed methane tanks". *International Journal of Thermal Sciences*, Vol. 48, No. 6, pp. 1176–1183.

Lima, J.A., Quaresma, J.N.N. and Macêdo, E.N., 2007. "Integral transform analysis of MHD flow and heat transfer in parallel-plates channels". *International Communications in Heat and Mass Transfer*, Vol. 34, pp. 420–431.

Monteiro, E.R., Macedo, E.N., Quaresma, J.N.N. and Cotta, R.M., 2009. "Integral transform solution for hyperbolic heat conduction in a finite slab". *International Communications in Heat and Mass Transfer*, Vol. 36, No. 4, pp. 297–303.

Naveira, C.P., Lachi, M., Cotta, R.M. and Padet, J., 2009. "Hybrid formulation and solution for transient conjugated conduction-external convection". *International Journal of Heat and Mass Transfer*, Vol. 52, No. 1-2, pp. 112–123.

Naveira-Cotta, C.P., Cotta, R.M., Orlande, H.R.B. and Fudym, O., 2009. "Eigenfunction expansions for transient diffusion in heterogeneous media". *International Journal of Heat and Mass Transfer*, Vol. 52, pp. 5029–5039.

Patankar, S.V., 1980. *Numerical Heat Transfer and Fluid Flow*. Hemisphere.

Paz, S.P.A., Macedo, E.N., Quaresma, J.N.N. and Cotta, R.M., 2007. "Eigenfunction expansion solution for boundary-layer equations in cylindrical coordinates: simultaneously developing flow in circular tubes". *Numerical Heat Transfer, Part A: Applications*, Vol. 52, No. 12, pp. 1123–1149.

Sphaier, L.A. and Cotta, R.M., 2002. "Analytical and hybrid solutions of diffusion problems within arbitrarily shaped regions via integral transforms". *Computational Mechanics*, Vol. 29, No. 3, pp. 265–276.

Sphaier, L.A., Cotta, R.M., Naveira-Cotta, C.P. and Quaresma, J.N.N., 2011. "The unit algorithm for solving one-dimensional convection-diffusion problems via integral transforms". *International Communications in Heat and Mass Transfer*, Vol. 38, pp. 565–571.

9. RESPONSIBILITY NOTICE

The authors are the only responsible for the printed material included in this paper.